

Interfaces of Correlated Electron Systems: Proposed Mechanism for Colossal Electroresistance

Takashi Oka¹ and Naoto Nagaosa^{1,2,3}

¹*Correlated Electron Research Center (CERC), National Institute of Advanced Industrial Science and Technology (AIST), Tsukuba Central 4, Tsukuba 305-8562, Japan*

²*Department of Applied Physics, University of Tokyo, Bunkyo-ku, Tokyo 113-8656, Japan*

³*CREST, Japan Science and Technology Corporation (JST), Saitama, 332-0012, Japan*

(Received 2 September 2005; published 23 December 2005)

Mott's metal-insulator transition at an interface due to band bending is studied by the density matrix renormalization group approach. We show that the result can be recovered by a simple modification of the conventional Poisson's equation approach used in semiconductor heterojunctions. A novel mechanism of colossal electroresistance is proposed, which incorporates the hysteretic behavior of the transition in higher dimensions.

DOI: [10.1103/PhysRevLett.95.266403](https://doi.org/10.1103/PhysRevLett.95.266403)

PACS numbers: 71.30.+h, 71.10.Fd, 73.40.-c

A strongly correlated electron system (SCES)—a group of materials in which the effect of Coulomb repulsion is large—is one of the major candidates on which the next-generation electronics may be built [1–8]. This strong hope put onto SCES electronics stems from the richness of its phase diagram [9]: Various electronic and magnetic phase transitions are reported with high sensitivity to external conditions. Inside electric devices, the electrons behave collectively, so the high sensitivity of SCES may lead to drastic functionalities.

Yet, SCES electronics faces a strong conceptual barrier to widespread acceptance and application, since it is essentially many body where the useful concepts such as band structure are believed to fail. It is expected to be the case especially at the interfaces. In this Letter, we study *interface Mott transition* near an interface between a metal electrode and SCES in terms of the density matrix renormalization group (DMRG) method [10]. Surprisingly, we found that the conventional band bending picture based on Poisson's equation is valid with a small modification [Eq. (3)]. Namely, the conventional concepts in semiconductor devices are still useful and valid to design the SCES devices. As an application, we propose a novel mechanism of the colossal electroresistance (CER), i.e., the large switching of resistance.

Among many possibilities for industrial applications, perhaps CER in SCES heterostructures is closest to realization, e.g., nonvolatile resistance random access memories (RRAM) [1]. The device consists of a film of perovskite manganite such as $\text{Pr}_{1-\delta}\text{Ca}_\delta\text{MnO}_3$, $\delta = 0.3$ (PCMO), which is a hole-doped Mott insulator, sandwiched by two metallic electrodes. The current-voltage curve shows large hysteresis at room temperature, where the resistivity of the on and off states differ by a large factor. Although this effect has been explored in details [2–6], the understanding of the mechanism is still missing. Baikalov *et al.* pointed out from multilead resistance measurements that the switching takes place at the interface [5]. Then, Sawa *et al.* reported that the CER behavior depends on the work function of the electrode metal [6].

They interpreted the I - V characteristics using a Schottky contact model (metal or p -type semiconductor) accompanied with an interface state. Another mechanism was proposed by Rozenberg *et al.* [11].

The mechanism of CER we propose here does not assume any interface states but attributes the large non-linearity of the I - V characteristics to interface Mott transition, where a layer of Mott insulator blocks the current. In dimensions higher than one, the transition is first order, and the width of the Mott insulator layer depends on how the voltage is changed. This explains the hysteretic behavior of the I - V characteristics.

The Letter consists of two parts. We first study a one-dimensional model of a metal-SCES interface using DMRG combined with Poisson's equation. We show that interface Mott transition can be understood on the basis of local equilibrium, i.e., the electric state is determined by the local value of the potential. Then, we explore the hysteresis loop of the I - V characteristics on a phenomenological basis assuming the hysteretic density-potential curve for a system in higher dimensions. Along with the mechanism of CER, another interesting consequence of interface Mott transition is proposed: A *quantum well* structure emerges spontaneously [Fig. 1(a)] at the interface of a hole (electron) doped Mott insulator and an electrode with a small (large) work function. Our results may lead to fabrication of clean 2D metallic systems analogous to the high electron mobility transistor in semiconductor physics.

DMRG study of a 1D interface.—We start with the one-dimensional model of a metal-SCES interface on a lattice with total Hamiltonian

$$H_{\text{tot}} = H_{\text{elc}} + H_{\text{SCES}} + H_{\text{jnc}}, \quad (1)$$

where the electrode $H_{\text{elc}} = -t \sum_{\sigma} \sum_{i=1}^{L/2-1} (c_{i+1\sigma}^{\dagger} c_{i\sigma} + \text{H.c.})$ and SCES $H_{\text{SCES}} = -t \sum_{\sigma} \sum_{i=L/2+1}^{L-1} (c_{i+1\sigma}^{\dagger} c_{i\sigma} + \text{H.c.}) + \sum_{i=L/2+1}^L (U n_{i\uparrow} n_{i\downarrow} + V_i n_i)$ is connected by a junction $H_{\text{jnc}} = -t \sum_{\sigma} (c_{L/2+1\sigma}^{\dagger} c_{L/2\sigma} + \text{H.c.})$. t is the hopping element, L the total size of the system with the interface at the center, and U denotes the on-site Coulomb repulsion (for a

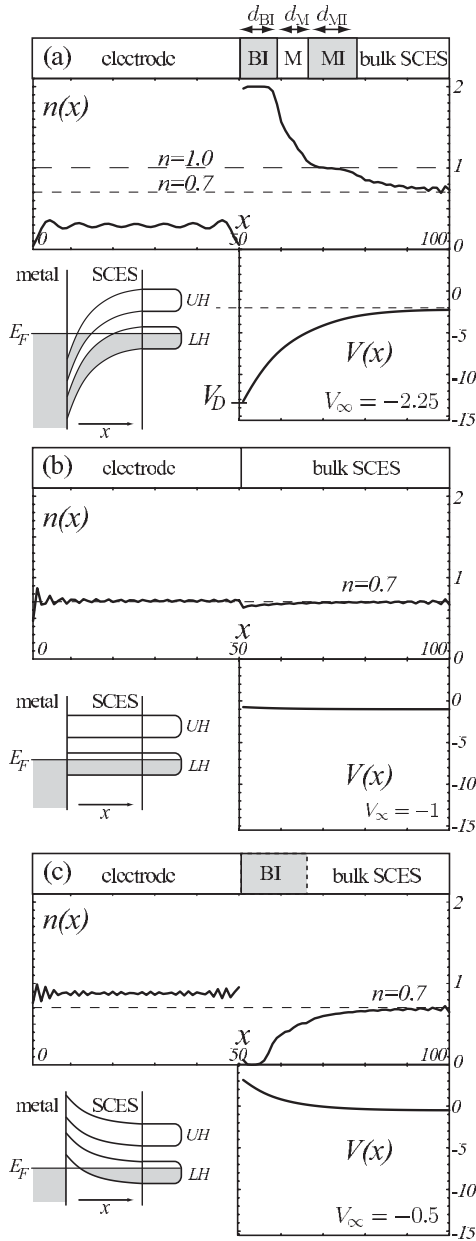


FIG. 1. Electron density $n(x)$ (upper panel) and potential $V(x)$ (lower panel) in a metal-SCES interface with (a) $V_\infty = -2.25$, (b) $V_\infty = -1$, and (c) $V_\infty = -0.5$ ($U/t = 4$, $n_+ = 0.7$, $\alpha = 0.043$, and $L = 100$). In each panel, a description of each region is given in the top where dark (white) regions are insulator (metal), e.g., band insulator (BI), metal (M), and Mott insulator (MI). The schematic picture in the left-lower space describes the bending of the upper (lower) Hubbard band UH (LH) near the interface. E_F is the Fermi energy.

related work, see [12]). We take the units $\hbar = \varepsilon_0 = 1$. The potential V_i defined in the SCES region obeys the 1D Poisson's equation, whose discretized solution is

$$V_i = -\alpha \sum_{j=i}^L \sum_{l=j}^L (n_l - n_+) + V_\infty, \quad i \in [L/2 + 1, L], \quad (2)$$

where $n_l = \langle \sum_{\sigma} c_{l\sigma}^\dagger c_{l\sigma} \rangle$ is the electron density and n_+ the

positive background related to the hole doping ratio δ by $n_+ = 1 - \delta$, and $\alpha = \frac{e}{\varepsilon a}$ (a , lattice constant; ε , dielectric constant). $[a, b]$ stands for the interval between a and b . H_{SCES} , without V_i , is identical to the Hamiltonian of the one-dimensional Hubbard model, which exhibits a Mott transition at half-filling if $U > 0$ [13]. If $n \neq 1$, the ground-state is metallic, a state known as the Tomonaga-Luttinger liquid (e.g., [14]).

The DMRG calculation is performed as follows. In order to obtain the ground-state consistent with the potential determined by Poisson's equation, we update the potential using Eq. (2) at each step of the finite size method in the DMRG procedure [10]. This is repeated more than 50 times to obtain total convergence. The typical size of the block Hilbert space used here is $m = 250$. We fix the total number of electrons $\sum_{i=1}^L n_i = Ln_+$; thus, the Fermi level of the electrode changes as electrons (holes) are injected to the SCES region when we vary V_∞ . The interface is characterized by the work-function difference $V_D \equiv (\text{work function of electrode}) - (\text{work function of SCES}) = (\text{potential bending}) = V_{L/2+1} - V_L$. We note that V_∞ achieving a given V_D depends on L .

In Fig. 1, we plot the electron density and the potential in a metal-SCES interface. Three typical solutions are plotted in an increasing order of V_D from (a) to (c).

(a) Interface Mott transition: When the electrode's work function is small enough, a quantum well is formed at the interface, i.e., two insulating [Mott insulator (MI) and band insulator (BI)] layers with widths d_{MI} and d_{BI} sandwich a metallic (M) region with width d_{M} . The V_D dependences of these widths are plotted in Fig. 2(b).

(b) Ohmic junction: The Fermi surface of the electrode and SCES balances, and no barrier is formed.

(c) Schottky barrier: A Schottky barrier is formed as in conventional metal-semiconductor interfaces.

It is noted here that the qualitative features of the results are all captured well by the conventional band bending picture by replacing the valence (conduction) band by the lower (upper) Hubbard band as shown in Fig. 1. We also note that in the three cases, $n(x)$ shows an oscillatory behavior in the electrode regime, which is the 1D Friedel oscillation $\delta n(x) = \cos(2k_F r + \eta_F)/r$ with k_F the Fermi wave number, η_F a phase shift, and r the distance from the interface.

In Fig. 2(a), we plot the electron density $n(x)$ against $-[V(x) - V_\infty]$ in the SCES regime ($x \in [51, 90]$), where data near the boundary ($x \in [91, 100]$) were omitted to avoid the boundary effect. The data fall onto a universal density-potential curve, which increases as the potential becomes deeper. In the middle of the curve, there is a plateau at half-filling whose width is $\Delta(U)$. The interface Mott transition is an analog of the filling driven Mott transition [15,16]. There the filling $n(\mu)$ of a grand canonical system is studied while the chemical potential μ is varied. The universal density-potential curve is an analog of the $n(\mu)$ curve in the filling driven Mott transition,

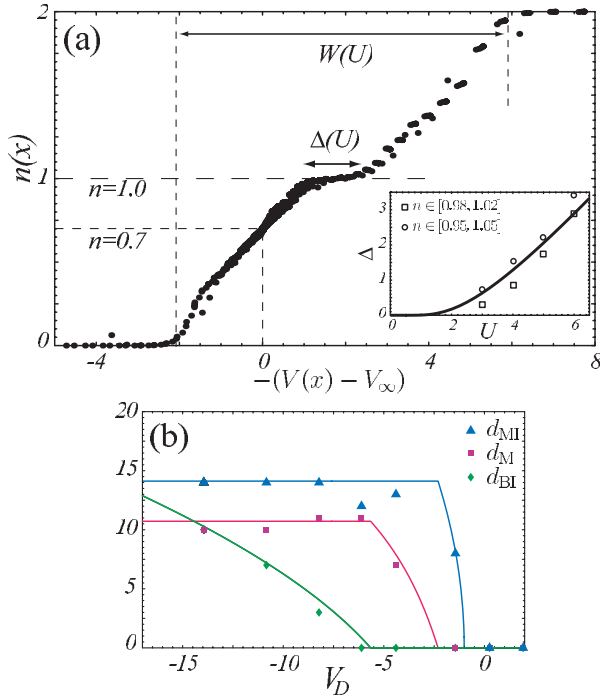


FIG. 2 (color). (a) Universal density-potential relation of the 1D interface Mott transition. Electron density $n(x)$, $51 \leq x \leq 90$ is plotted against $-[V(x) - V_\infty]$. V_∞ is varied from $V_\infty = -3.00$ to $V_\infty = 0$ with an interval of 0.25. $W(U)$ is the bandwidth and $\Delta(U)$ the width of the $n = 1$ plateau. Inset: The U dependence of $\Delta(U)$. This is determined from data with density $n \in [0.96, 1.04]$ (open circle) and $n \in [0.98, 1.02]$ (open boxes). The solid line is the Mott gap from Lieb-Wu's solution [13]. (b) The width of the Mott insulating (d_{MI} , $n \in [0.85, 1.04]$; blue), metallic (d_M , $n \in [1.04, 1.96]$; red) and band insulating (d_{BI} , $n \in [1.96, 2.0]$; green) layers plotted against V_D . The symbols are DMRG results while the solid lines are the solutions of Poisson's equation [Eqs. (4)–(6)].

where $-V(x)$, with a shift of the zero point, plays the role of μ . Indeed, when we compare the width of the plateau

$$d_M = \sqrt{\varepsilon/\varepsilon\kappa} \cosh^{-1} \left[\frac{\{(V_D + \Delta)\delta/\kappa + \sqrt{2\Delta\delta/\kappa} \sqrt{(V_D + \Delta + \delta/\kappa)^2 - 2(\delta/\kappa)(V_D + \delta/\kappa)}\}}{\{2\Delta\delta/\kappa - (\delta/\kappa)^2\}} \right], \quad (5)$$

which saturates when $V_D < -\frac{1+\delta}{\kappa} - \Delta$. Finally, the width of the BI layer is nonzero when $V_D < -\frac{1+\delta}{\kappa} - \Delta$

$$d_{BI} = \frac{-F_2 + \sqrt{(F_2)^2 - 2\frac{\varepsilon}{\varepsilon}(1+\delta)((1+\delta)/\kappa + V_D + \Delta)}}{\frac{\varepsilon}{\varepsilon}(1+\delta)} \quad (6)$$

with $F_1 = \sqrt{2e\Delta\delta/\varepsilon}$ and $F_2 = F_1 \cosh(\sqrt{e\kappa/\varepsilon}d_M) + \sqrt{e\kappa/\varepsilon} \frac{\delta}{\kappa} \sinh(\sqrt{e\kappa/\varepsilon}d_M)$ where d_M here is obtained by substituting $V_D = -\frac{1+\delta}{\kappa} - \Delta$ in Eq. (5). In Fig. 2(b), we plot the V_D dependence of the widths and compare them with the DMRG results, and both agree surprisingly well. This agreement is highly nontrivial: In the insulating phase the localization length $\xi \sim W/\Delta(U)$ is of the order of few sites, but in the metallic phase it should diverge. So, in the

with the Lieb-Wu solution of the Mott gap of the one-dimensional Hubbard model $\Delta(U) = \frac{16t}{U} \int_1^\infty \frac{\sqrt{y^2-1}}{\sinh(2\pi y t/U)} dy$ [13], the two coincide well as shown in the inset of Fig. 2(a). Thus, it can be said that the density-potential relation in the interface Mott transition follows the $n(\mu)$ curve in the bulk transition.

Poisson's equation and local equilibrium approximation.—Since the metal-SCES interface determines the transport properties of the device, the width of the layers d_{MI} , d_M , and d_{BI} in Fig. 1(a) is of practical interest. Here, we derive the width by solving the modified Poisson's equation

$$\frac{d^2V(x)}{dx^2} = -\frac{e}{\varepsilon} [n(V(x)) - n_+], \quad (3)$$

where we assume local equilibrium, that is, we assume that the electron density depends only on the local value of the potential. In the following, we evaluate Eq. (3) to obtain the widths expressed solely by the potential difference V_D , hole doping ratio δ , bandwidth W , and the Mott gap Δ .

We adopt a simplified density-potential relation by linearizing the DMRG result Fig. 2(a): A constant compressibility $-dn(V)/dV = \kappa \equiv 2/(W - \Delta)$ is assumed for $-[V(x) - V_\infty] \in [(\delta - 1)/\kappa, \delta/\kappa]$, $[\delta/\kappa + \Delta, (1 + \delta)/\kappa + \Delta]$, and $n(V) = 0$ for $-[V(x) - V_\infty] \in [-\infty, (\delta - 1)/\kappa]$, $n(V) = 1$ for $-[V(x) - V_\infty] \in [\delta/\kappa, \delta/\kappa + \Delta]$, and $n(V) = 2$ for $-[V(x) - V_\infty] \in [(1 + \delta)/\kappa + \Delta, \infty]$. We seek a solution with a fixed density at the bulk SCES $n(x) = n_+ = 1 - \delta$, MI layer $n(x) = 1$ and BI layer $n(x) = 2$, but varies in the metallic region (M). The width of the MI layer is nonzero when $V_D < -\delta/\kappa$

$$d_{MI} = \sqrt{2\varepsilon(-V_D - \delta/\kappa)/e\delta} \quad (4)$$

and saturates at $V_D = -\delta/\kappa - \Delta$. When the MI layer saturates, the metallic region appears whose width is

metallic phase the local approximation is not *a priori* justified. However, our numerical calculation shows that it works remarkably well. Based on this success, we apply this local approximation to more generic cases below.

Application to CER.—In CER devices, the interface between the electrode and SCES is two dimensional. In systems with dimensions higher than one, the filling driven Mott transition is first order, and hysteretic behavior takes place near the transition point [15–17]. We expect similar hysteresis in the density-potential relation of the interface Mott transition [Fig. 3(a)]. If this is the case, coexistence of the metallic state and the insulating state is possible. Then, the I - V characteristics of the device shows high nonlinearity as well as a memory effect, i.e., RRAM behavior, when a layer of the coexistence state exists in the SCES

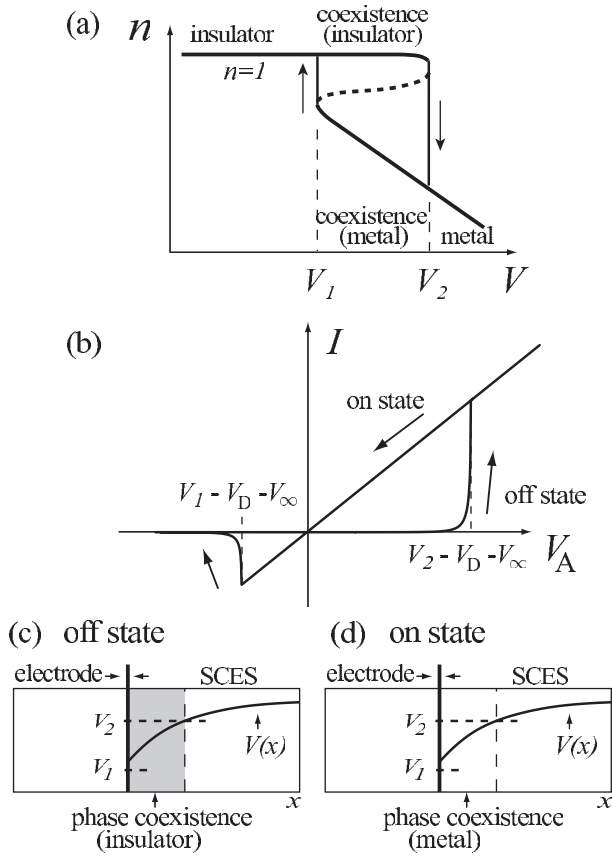


FIG. 3. (a) Density-potential relation near Mott's transition in dimensions higher than one (schematic). A region ($V_1 < V < V_2$) exists where metallic and insulating phases coexist. (b) I - V characteristics of the metal-SCES interface when $V_1 < V_D + V_\infty < V_2$ is satisfied. Pictures of the off state (c) and on state (d).

region. The condition for this to take place is $V_D < -(\delta - \Delta\delta_1)/\kappa$. For example, if $V_1 < V_D + V_\infty < V_2$ is satisfied, the region nearest the interface is a phase coexistence layer, as shown in Figs. 3(c) and 3(d). If this is the case, the junction may be insulating 3(c) or metallic 3(d). They correspond to the off and on states, respectively. We can switch between them by applying a voltage V_A on the electrode, forming a hysteresis loop in the I - V characteristics Fig. 3(b). We assume a tunneling form for the current

$$I(V_A) = T(V_A)I_0(V_A), \quad (7)$$

where $T(V_A)$ is the tunneling probability of the barrier and $I_0(V_A)$ the current at the metal-SCES junction without any barrier. $I_0(V_A)$ reflects the details of the device and may be Ohmic, i.e., $I_0(V_A) \propto V_A$, or if space charge limited current is realized, $I_0(V_A) \propto (V_A)^2$ [18]. We assume that the tunneling probability decreases exponentially as the width of the MI layer grows, i.e., $T(V_A) = e^{-d_{\text{MI}}(V_A)/\xi}$, where ξ is the decay length (here the temperature dependence is neglected). Neglecting the jump of n in Fig. 3(a), the width of the MI layer can be obtained by replacing $-V_D - \delta/\kappa$ in Eq. (4) with $V_i - V_D - V_\infty - V_A$, $i = 1, 2$ for the on and off states, respectively. Thus, a hysteresis loop is realized

in the I - V characteristics as in Fig. 3(b). If we define the CER ratio by $\Delta R/R \equiv (R_{\text{off}} - R_{\text{on}})/R_{\text{on}}$, where $R_{\text{on,off}}$ is the resistivity of the on and off states, we obtain $\Delta R/R = e^{\sqrt{2\varepsilon(V_2 - V_D - V_\infty)/e\delta}/\xi} - 1$. In a Ti/PCMO based CER device, however, neither the on nor the off states show Ohmic I - V characteristics [6]. This can also be understood by our model with $V_D + V_\infty < V_1$. In such cases, the CER ratio becomes $\Delta R/R = e^{\sqrt{2\varepsilon(V_2 - V_D - V_\infty)/e\delta} - \sqrt{2\varepsilon(V_1 - V_D - V_\infty)/e\delta}}/\xi} - 1$. In either case, we can design a CER device with larger CER ratio by decreasing the doping ratio δ and making the phase coexistence region wider.

In summary, we have studied the interface Mott transition by the DMRG method and by Poisson's equation combined with a local equilibrium ansatz. We proposed a novel mechanism of CER for materials with a first order metal-insulator transition. An important future problem is to extend the DMRG analysis to ladder and higher dimensional systems and clarify the conditions for the hysteresis behavior.

We acknowledge illuminating discussions with A. Sawa, I. H. Inoue, M. Kawasaki, and Y. Tokura. We also thank Y. Ogimoto for careful reading of the manuscript. T. O. acknowledges S. Onoda and F. Ogushi for helpful comments.

- [1] A. Asamitsu, Y. Tomioka, H. Kuwahara, and Y. Tokura, *Nature* (London) **388**, 50 (1997).
- [2] V. Ponnambalam, S. Parashar, A. R. Raju, and C. N. R. Rao, *Appl. Phys. Lett.* **74**, 206 (1999).
- [3] H. Oshima, K. Miyano, Y. Konishi, M. Kawasaki, and Y. Tokura, *Appl. Phys. Lett.* **75**, 1473 (1999).
- [4] S. Q. Liu, N. J. Wu, and A. Ignatiev, *Appl. Phys. Lett.* **76**, 2749 (2000).
- [5] A. Baikalov *et al.*, *Appl. Phys. Lett.* **83**, 957 (2003).
- [6] A. Sawa, T. Fujii, M. Kawasaki, and Y. Tokura, *Appl. Phys. Lett.* **85**, 4073 (2004).
- [7] T. Hasegawa, K. Mattenberger, J. Takeya, and B. Batlogg, *Phys. Rev. B* **69**, 245115 (2004).
- [8] A. Ohtomo and H. Y. Hwang, *Nature* (London) **427**, 423 (2004).
- [9] M. Imada, A. Fujimori, and Y. Tokura, *Rev. Mod. Phys.* **70**, 1039 (1998).
- [10] S. R. White, *Phys. Rev. Lett.* **69**, 2863 (1992).
- [11] M. J. Rozenberg, I. H. Inoue, and M. J. Sánchez, *Phys. Rev. Lett.* **92**, 178302 (2004).
- [12] K. Yonemitsu, *J. Phys. Soc. Jpn.* **74**, 2544 (2005).
- [13] E. H. Lieb and F. Y. Wu, *Phys. Rev. Lett.* **21**, 192 (1968).
- [14] H. Schulz, *Correlated Electron Systems*, edited by V. J. Emery (World Scientific, Singapore, 1992).
- [15] D. S. Fisher, G. Kotliar, and G. Moeller, *Phys. Rev. B* **52**, 17112 (1995).
- [16] G. Kotliar, S. Murthy, and M. J. Rozenberg, *Phys. Rev. Lett.* **89**, 046401 (2002).
- [17] S. Onoda, cond-mat/0408207.
- [18] M. A. Lampert and P. Mark, *Current Injection in Solids* (Academic Press, New York, 1970).